We are IntechOpen, the world's leading publisher of Open Access books Built by scientists, for scientists

6,900
Open access books available

185,000
International authors and editors

200M
Downloads

154
Countries delivered to

Our authors are among the

TOP 1%
most cited scientists

12.2%
Contributors from top 500 universities

CLARIVATE ANALYTICS

BOOK CITATION INDEX

INDEXED

WEB OF SCIENCE™

Selection of our books indexed in the Book Citation Index
in Web of Science™ Core Collection (BKCI)

Interested in publishing with us?
Contact book.department@intechopen.com

Numbers displayed above are based on latest data collected.
For more information visit www.intechopen.com

Improvement of Critical Current Density and Flux Trapping in Bulk High-T_c Superconductors

Mitsuru Izumi and Jacques Noudem

Additional information is available at the end of the chapter

1. Introduction

The present chapter describes an overview of flux trapping with enhancement of the critical current density (J_c) of a melt-growth large domain $(RE)Ba_2Cu_3O_{7-d}$, where RE is a light rare earth ions such as Y, Gd or Sm. These high-T_c superconductor bulks have attracted much interest for a variety of magnet applications, since high density and large volume materials potentially provide an intensified magnetic flux trapping, thanks to the optimized distribution of pinning centres. The melt growth process and material processing to introduce well-defined flux pinning properties are overviewed. As a first step, we summarize an effort to achieve a growth of homogeneous large grains with the second phase RE211 in the RE123/Ag matrix. RE-Ba-Cu-O material has a short coherence length and a large anisotropy, and thus any high-angle grain boundary acts as a weak link and seriously reduces the critical current density [1, 2]. In engineering applications, high texture and c-axis-orientated single grains/domains are required. Large-sized, high-performance RE-Ba-Cu-O single grains are now commercially available. The trapped flux density (B_{trap}) due to flux pinning or associated superconducting currents flowing persistently in a RE-Ba-Cu-O grain is expressed in a simple model, such as:

$$B_{trap} = A\mu_0 J_c r,$$

where A is a geometrical constant, μ_0 is the permeability of the vacuum and r is the radius of the grain [1]. There are two approaches to enhancing the trapped flux of the grain. One is to enhance the critical current density and the other is to increase the radial dimension of the crystals. Increasing the dimension requires the formation of homogeneous grain growth, and the enhancement of the critical current density is encouraged with the improvement of flux pinning properties.

The top-seeded melt-growth (TSMG) method has been widely used to fabricate large, single-grain RE-Ba-Cu-O superconducting bulks that show a considerable ability in

magnetic flux trapping and great potential for large-scale applications [1]. Hot seeding and cold seeding procedures have been studied. For hot-seeding processes, Nd-Ba-Cu-O or Sm-Ba-Cu-O crystals with a high decomposition temperature are put on the matrix during the growth of the bulk, around a peritectic temperature (T_P), which is not convenient for the batch process and often brings problems for reproducibility. Cardwell et al. have introduced a cold-seeding process with Mg-doped Nd-Ba-Cu-O crystals as generic seeds whose decomposition temperature is higher than the pure substance [3, 4]. Nd-Ba-Cu-O and Sm-Ba-Cu-O thin films grown on MgO substrates have been examined as cold seeds [5, 6]. Thanks to the superheating phenomenon of Nd-Ba-Cu-O thin films, the maximum temperature (T_{max}) is increased up to even 1090 °C [7, 8]. Muralidhar et al. have reported a batch process of Gd-Ba-Cu-O bulks [9, 10]. Recently, it has been reported that a buffer pellet inserted between the seed and the matrix effectively suppresses the chemical contamination caused by the dissolution of the seed, without affecting the texture growth, and the T_{max} is increased to 1096 °C [8, 11].

An idea for the novel cold-seeding of a top-seeded melt-growth with a RE-Ba-Cu-O bulk has been worked on by employing an MgO crystal seed and a buffer pellet [12]. The growth process is composed of two stages. The MgO seed was for the texture-growth of the small RE-Ba-Cu-O pellet with a high melting point (T_P), and the textured pellet induced the texture growth of the bulk at a lower temperature. Undercooling and the RE211 content of the pellet were adjusted to avoid the misorientation caused by lattice mismatch between MgO and the RE-Ba-Cu-O matrix. Bulk samples prepared with this method show good growth sections and superconducting performance. One of the promising advantages of this method is in the processing of high T_P RE-Ba-Cu-O bulks with a cold seeding method, for example Nd-Ba-Cu-O bulks.

Detailed information for the preparation of the samples is described elsewhere [12]. $GdBa_2Cu_3O_{7-\delta}$ (3N, Gd123), Gd_2BaCuO_5 (3N, Gd211) powders were employed with 40 mol% of Gd211 for Gd123. 10 wt.% Ag_2O and 0.5 wt.% Pt were added. A small buffer pellet of Gd123 contained a certain amount of Gd211. A single (100)-oriented MgO seed was placed onto the small pellet.

According to the results of the differential thermal analysis (DTA) measurements [12], we used the heat treatment profile shown in Fig. 1. The sample was heated within 10 hours to T_{max}, 90 °C higher than the $T_{P\text{-matrix}}$ (for the matrix with the addition of Ag_2O). After one hour, the temperature was reduced to $T_{P\text{-buffer}} - \Delta T$ within 30 minutes so as to begin the growth of the buffer pellet. ΔT stands for the undercooling. After that the temperature was reduced over 30 minutes to $T_{P\text{-matrix}}$ and further slowly decreased by 30 °C with a cooling rate of 0.3 °C/h. Eventually, the temperature was decreased to room temperature within 10 hours. The following post-annealing process has been reported in our previous studies [13, 14].

Fig. 2 shows the appearance of the bulk samples prepared by conventional hot-seeding (a), cold-seeding using a Nd123 thin film (b), and cold-seeding in association with a MgO-buffer pellet (c). The c-axis oriented single-grain growth for the buffer pellet is of importance. Cardwell et al. and Babu et al. have reported that the geometry of Nd-Ba-Cu-O single grains, texture-processed by MgO seeds, will vary from rectangular ($\Delta T < 10$ °C) to

rhombohedral (high values of ΔT) under different growth temperatures [15, 16] Cima et al. have demonstrated that the so called "faced plane growth front" type of solidification interface morphologies is largely dependent on the growth rate [17]. The undercooling is directly related to the growth rate. Meanwhile, the RE211 content affects the growth rate. A slow cooling between 1030 °C and 1025 °C with 10 mol % Gd211 content is suitable for the buffer pellet's texture growth.
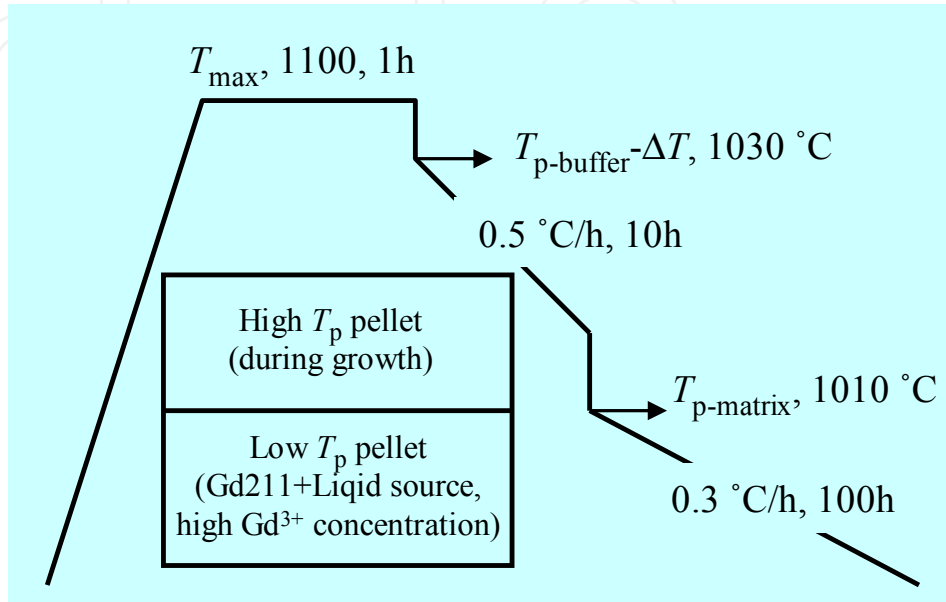

Figure 1. Schematic illustration of thermal profile for the cold-seeding growth of Gd-Ba-Cu-O bulk superconductors [12].

The present cold-seeding method can be used for growth with a high T_P bulk in the air, for example in a Nd-Ba-Cu-O bulk. The same progress for detecting a suitable undercooling and Nd422 content has been carried out in the Nd-Ba-Cu-O system. A slow cooling between 1067 °C and 1062 °C with rate of 0.5 °C/h and 10 mol% Nd422 content have been proven to offer the best growth conditions for the Nd-Ba-Cu-O buffer pellet [12].

The growth can be transferred from a high-T_P pellet to a low-T_P pellet. As illustrated in Fig. 1, during the growth of the high-T_P part, the low-T_P part is kept at a relatively high temperature, which means that a high RE concentration may exist. It is promising for extending the growth window and benefits of a larger scale bulk superconductor from the viewpoint of homogeneity. The addition of silver as well as the mixture of two or three kinds of RE123 powders may change T_P. Recently, we have found that by doping 30 mol% Nd123 into the Gd123 precursor powders, the T_P is increased by 6 °C while keeping texture growth.

Fig. 3 shows the microstructure of the portion at the buffer/matrix interface. The boundary is denoted by the broken line. A different contrast of Gd211 density was observed below and above the boundary. Because of the push effect of Gd211, a high Gd211 density area is formed at the interface. The composition of the matrix was measured by EPMA for points indicated by green closed circles in Fig. 3 (a). There is $Gd_{1+0.02}Ba_{2-0.02}Cu_{2.72}$ in the composition

of the buffer side and it is approximately close to $Gd_{1+0.09}Ba_{2-0.09}Cu_{2.64}$ in the matrix side. We suspect that because of the large undercooling and growth rate, the Gd/Ba substitution is inhibited at the buffer side.
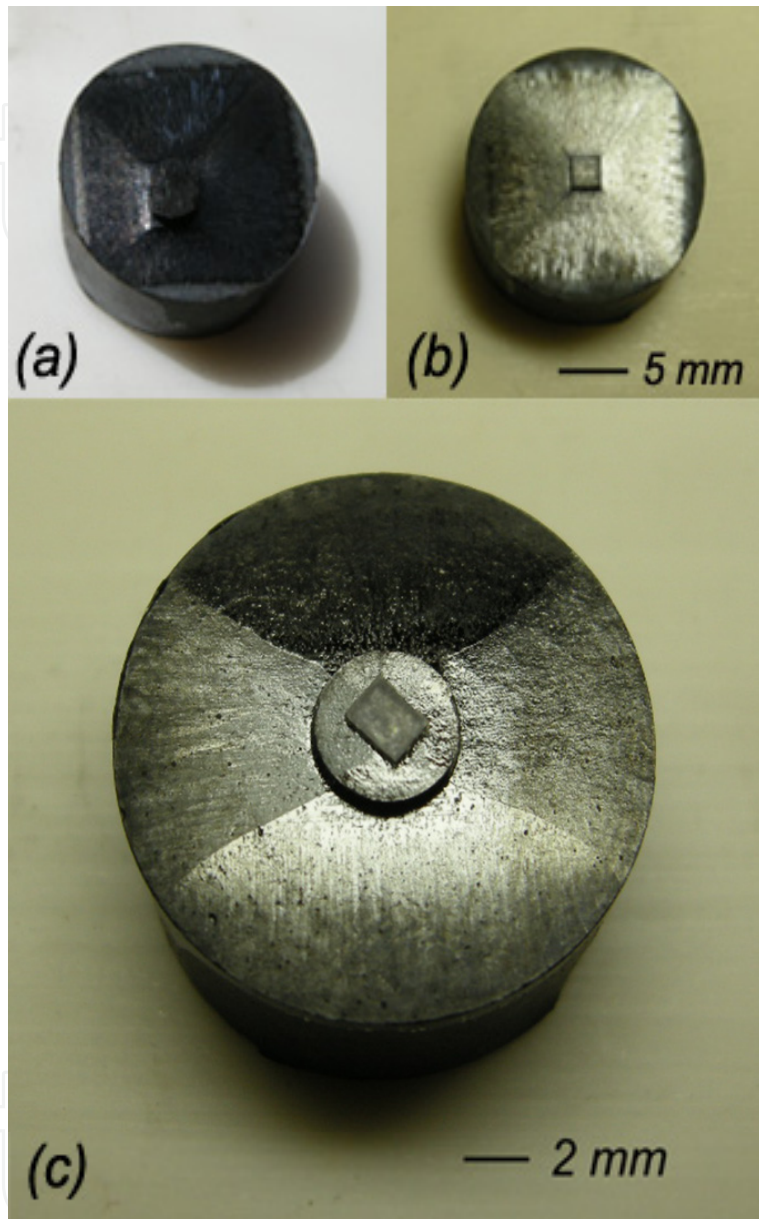

Figure 2. Gd-Ba-Cu-O single-grain bulk of 16 mm in diameter prepared by (a) a hot-seeding process, (b) a cold-seeding process using a Nd123 thin film seed, (c) a cold-seeding growth with a MgO crystal seed and a buffer pellet [12].

Secondly, we emphasize how to launch additional pinning centres into the RE123/Ag matrix. There are several strategies which are partly analogue to the implantation of pinning centres in thin film forms. Partial atomic substitutions of the Ba^{2+} site with RE^{3+} in RE123 induce a so-called "peak effect" around 1.5-2.0 T in the J_c-B curves. The substitution of 1D Cu site in the RE123 structure with other ions results in an enhanced peak effect [18]. Many kinds of additions of non-superconducting metal oxides have been studied in the Gd123 /Ag
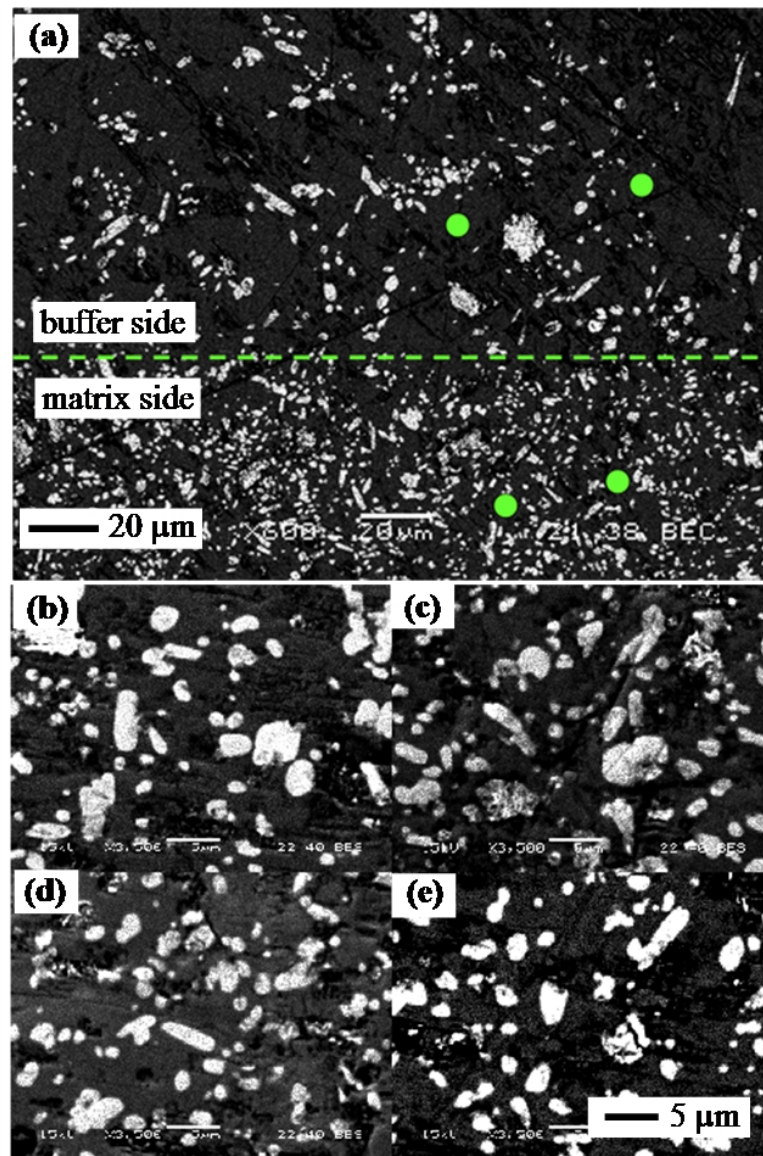
Figure 3. The microstructure of Gd-Ba-Cu-O bulk sample processed by a cold-seeding method using a MgO-buffer pellet observed by SEM. (a) Buffer/matrix interface, (b) C1: under the seed, (c) B1: periphery in the growth sector, (d) C4 position [12], (e) B4 position [12].

matrix with Gd211. Gd211 tends to form domains of a large size inside Gd123. Various kinds of oxides and $RE_2Ba_4MCuO_{11}$ (RE2411 particles, M = Zr, U, Mo, W, Ta, Hf, Nb) are introduced into the RE-Ba-Cu-O matrix as second phase particles so as to enhance flux pinning [19-20]. Up to now, the record of J_c reaches 640 kA/cm² and 400 kA/cm² at 77 K in the self field and 2 T, respectively. This record was achieved in the (Nd,Eu,Gd)-Ba-Cu-O bulk combining the benefits of dense regular arrays of a RE-rich RE123 solid solution, the initial Gd211 particles that were 70 nm in diameter and the formed small (< 10 nm) Nb (or Mo, Ti)-based nanoparticles [21]. Systematic research of the doping effect has been also carried out in our laboratory. J_c of 100 kA/cm², 68 kA/cm² and 80 kA/cm² were obtained at 77 K in a self field by doping with ZrO_2, ZnO and SnO_2 particles, respectively [22, 23]. It is interesting that the addition of nano-sized metal oxides - such as SnO and/or ZrO_2, for

example - provides not only the simple *in situ* formation of $BaSnO_3$ and $BaZrO_3$ but also the fining of the size of Gd211 distributed inside the matrix, as shown in Fig. 4. These effects are classified with the *in situ* formation of the nano-sized flux pinning centres during the growth process. To make for strong flux pinning, the introduction of nano-sized inclusions in textured bulk HTSs constitutes an effective means. Apart from making a fine second phase particle, dilute impurity doping is even more important for improving flux pinning. The increased Jc in such a dilute doping bulk is even several times larger than that in the reference sample. Therefore, at present, we focus on the chemical approach of dilute impurity doping. Different additives such as BaO_2, ZrO_2, ZnO, NiO, SnO_2, Co_3O_4, Fe_3O_4, Ga_2O_3 and Fe-B alloy [20, 22,23, 24-30], which lead to a slight decrease of T_c in the bulk RE-123, except for a few kinds of additives like Gd2411 and titanium oxide.
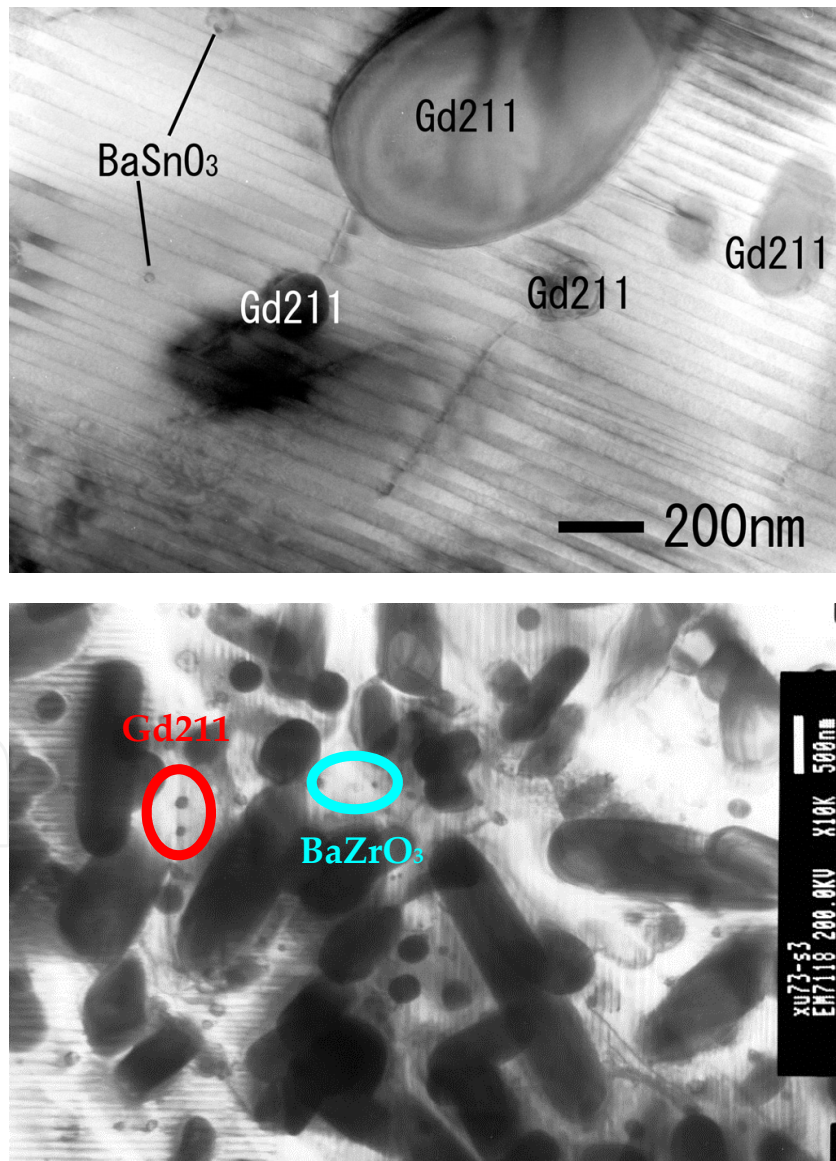

Figure 4. The microstructure of Gd-Ba-Cu-O bulk sample processed by the hot-seeding method observed by SEM. (a) ZrO_2 addition [22] and (b) SnO_2 addition [23].

Cardwell et al. [4] and Muralidhar et al. [10] have developed general process routes to grow batches of RE-Ba-Cu-O single domain superconductors with good pinning performance. The flux pinning and J_c performance of a RE-Ba-Cu-O bulk yield remarkable improvements by dispersing the non-superconducting secondary pinning phase into the RE-123 matrix. Successful attempts have been made to add nano-sized impurities [22, 23, 31], the fined RE-211s [32, 33] and Pt, Ce additives to prevent the Ostwald ripening of RE-211 inclusions into the precursors and to enhance flux pinning. On the other hand, compared with core pinning by normal non-superconducting particles, the use of ferromagnetic pinning centres results in interactions between a magnetic dipole moment and flux lines, which yields a potential Upin proportional to $-mb$, where m is the moment of magnetic dipole and b is the field of the vortex at the distance of the dipole [34]. The deeper potential wells may reduce the Lorentz force on the vortices [35-37].

Xu Yan et al. have found that Fe-B quenched amorphous magnetic alloy particles with small amounts of Cu-Nb-Si-Cr may be a useful additive for flux trapping properties [25, 26]. The results show that the J_c was enhanced under both low- and high-magnetic fields with the addition of 0.4 mol% of Fe-B particles [25, 26, 38].

SEM observations were also carried out to confirm the information of the Fe-rich region obtained from TEM. The representative back scattered electron image is shown in Fig. 5 (a), where the larger particles represent silver, and the homogeneous distributed small particles are Gd-211 embedded in the Gd-123 matrix, according to the EDX analysis. Consistent with the results from TEM, the Fe element was only found in the vicinity of silver, as shown in Fig. 5(b). This may be attributed to the following three reasons:

First, silver and Fe_3O_4 possess a cubic structure with a lattice mismatch: a = 8.397 A for Fe_3O_4 and a = 4.090 A for silver. Two unit cells of silver may be nearly equi-length with that of one unit cell of Fe_3O_4, giving a small lattice mismatch of 2.65%. Second, the oxidization temperature of Fe-B additives obtained in our DTA results is identified at around 960 °C, very close to the melting point of silver 961.9 °C. Meanwhile, the Fe-B additives were oxidized into Fe-containing components with porous structures, as confirmed by our experiment of annealing Fe-B alloy separately. As a result, the melted silver may fill these voids at high temperatures. Third, this oxidation process is an exothermal reaction, which accelerates the melting of adjacent silver particles. Fourth, the released oxygen from Ag_2O would be the source of the oxidization of Fe-B additives. The release of oxygen might provide a potential channel for the flowing of melted silver to Fe_3O_4. The advantage of the present materials process is in eliminating the proximity effect between magnetic Fe_3O_4 and the Gd-123 superconducting matrix by the silver as a buffer layer.

Besides this, in the growth process, the added Pt may exist around the boundary between Gd123 and Ag, for example. Fe is known to be with Ag. The addition of magnetic oxide, such as Fe_2O_3 or other kinds of Fe alloys, has been investigated from the viewpoint of the magnetic pinning effect. Tsuzuki et al. have reported that Fe_2O_3 was introduced into the Gd123 matrix [39]. The maximum trapped flux increased by over 30 %. In the case of Fe-B particles addition, J_c is increased in both center and edge of the samples. However, no

enhancement of J_c was observed at the edge with the Fe_2O_3 addition. Here, there is the difference of the integrated flux between Fe-B addition and Fe_2O_3 addition from the spatial distribution of J_c. The origin of homogeneous J_c and the effect of in-situ formation of Fe_2O_3 in the Fe-B added Gd123 bulks are the keys to improve the performance of the magnetic field trapping [40].

Separately, the optimal addition of these magnetic particles induces an increase of the number of Gd211 particles while decreasing the size. We emphasize the current issues concerning the homogeneity of the distribution of these particles together with TEM observations [38].
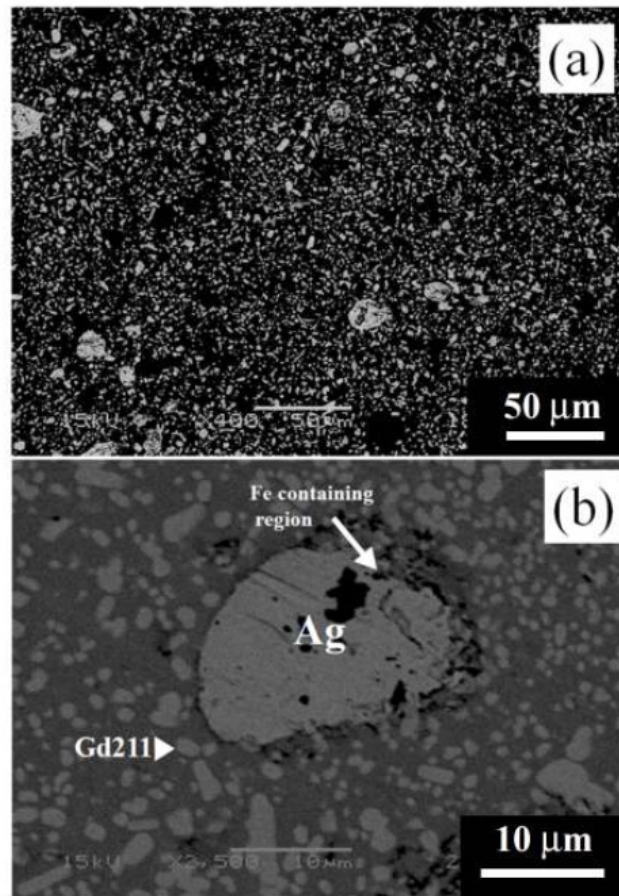

Figure 5. (a) Low magnification of an SEM image of a 1.4 mol% Fe-B doped Gd-Ba-Cu-O C1 specimen. (b) SEM image of a Fe-rich region [26].

Another unique aspect concerning flux trapping is to distribute holes drilled within the bulk pack. The recently reported [41-45] hole-patterned $YBa_2Cu_3O_y$ (Y123) bulks with improved superconducting properties are highly interesting from the points of view of material quality and their variety of application. It is well known that the core of plain bulk superconductors needs to be fully oxygenated, and some defects like cracks, pores and voids [46, 47] must be suppressed in order that the material can trap a high magnetic field or else carry a high current density. Some previous studies [48-51] demonstrated that, by filling

the cracks, enhancing thermal conductivity or by reinforcing the YBCO bulk material, the properties can be improved and a trap field of up to 17 T at 29 K can be reached. One of the interests of this new sample geometry is in increasing specific areas for thermal exchange, shortening the oxygen diffusion path, and offering the possibility of reinforcing the superconductor materials. To minimize the above defects, we propose the improvement of the superconducting material with an innovative approach - "material by design" based on the concept of a YBa$_2$Cu$_3$O$_y$ (Y123) bulk with multiple holes.
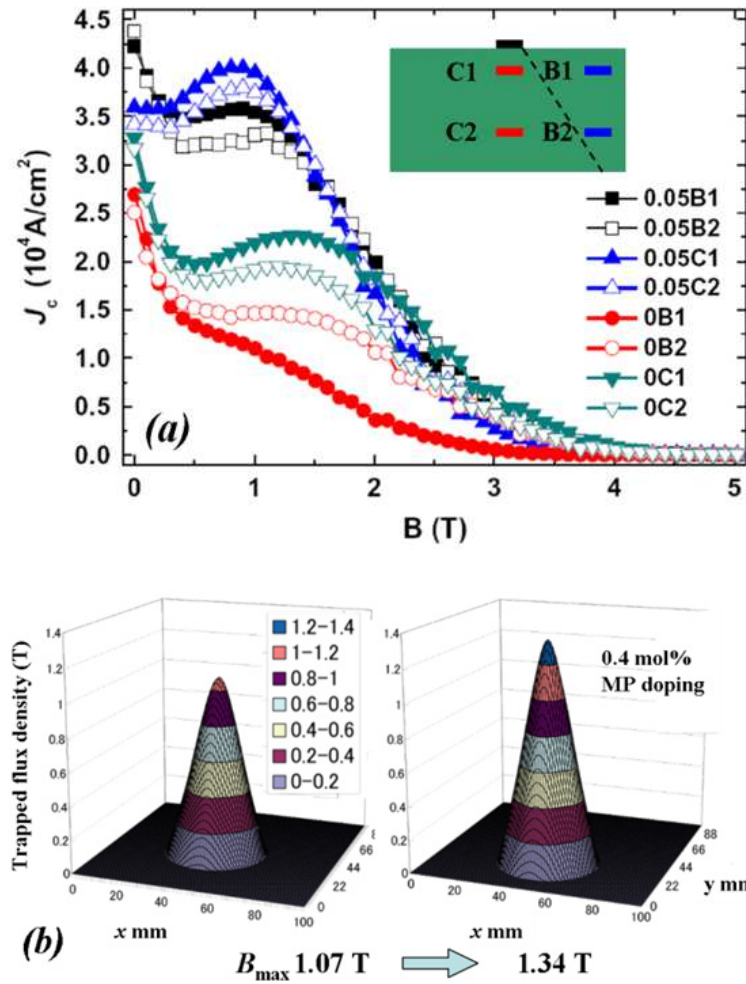

Figure 6. (a) The J_c-B curves of specimens cut from different positions of MP doped and un-doped bulk samples. (b) The trapped magnetic field of 46-mm MP-doped and un-doped bulks [25].

The details of the multiple holes process of YBa$_2$Cu$_3$O$_y$ (Y123) are reported elsewhere [41, 42]. Basically, the holes in the pre-sintered bulk were realized by drilling cylindrical cavities with different diameters, 0.5-2 mm through the circular or square shaped sample. The holes are arranged in a regular network on the plane of the samples. A SmBa$_2$Cu$_3$O$_x$ (Sm123) seed used as a nucleation centre was placed (between the holes close to the centre) on the top so as to obtain the single domain of the samples. The seed orientation was chosen to induce a growth with the c-axis parallel to the pellet axis. The elaboration of single domains through the drilled pellets is then conducted in a manner similar to the plain pellets. But how to

claim a single domain on the drilled sample? The demonstration of the growth of single domains from the perforated structure is shown by Fig. 7(a). The growth lines of faceted growth on the surface of the drilled single domain half are not clearly observed, but they exist when compared to the plain half. This shows that the pre-formed holes do not seem to
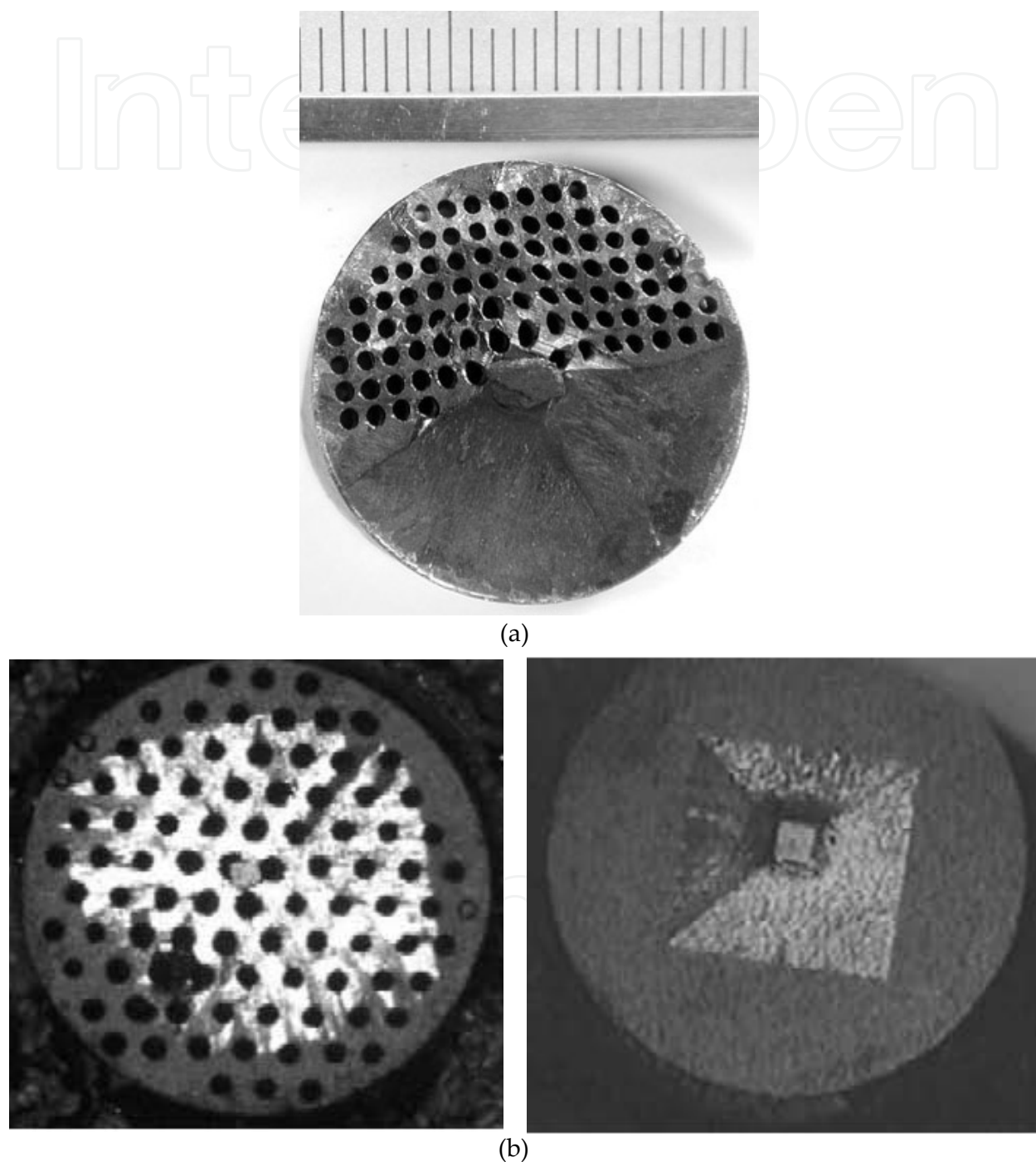

(a)

(b)

Figure 7. (a). Macrograph of the single domain pellet sample where only half has been drilled [44]. (b). Pictures of the surfaces of a drilled (left) and a plain (right) pellet taken at an intermediate stage of the growth process. The bright square is the growing domain with a seed at its centre. The steps and streaks result from the interaction of the holes with the growth front (left) [44].

disturb the growth of the single domain, which is confirmed by the top seed melt growth process of other perforated samples prepared by Chaud et al. [42]. Basically, the ability of a growth front to proceed through an array of holes or a complex geometry is not evident *a priori*. *In situ* video monitoring of the surface growth confirms that it proceeds as for a plain pellet. The growth starts from the seed. A square pattern typical of the growth front of the tetragonal Y123 phase in the a- and b- directions appears below the seed and increases homothetically until it reaches the edges of the sample. Intermediate pictures of the growth are shown in Fig. 7(b) for a drilled pellet (left) and for a plain pellet (right). The square pattern is distinguishable in both cases with the seed at its centre. Note that the seeds were cut with edges parallel to the a- or b- directions, which is why they coincide with the growing domain borders.

The various square or circular-shaped Y123 were grown into a single domain including an interconnected structure. Optical macrographs of as-grown samples with holes are shown in Fig. 8. Fig. 9 (a and b) illustrate the cross sections of plain and perforated samples. The porosity is drastically reduced for the drilled sample. For the plain sample, a large porosity and crack zones are noticeable. Scanning Electron Microscopy between two holes shows (i) the compact, crack–free microstructure and (ii) a uniform distribution of fine Y211 particles into the Y123 matrix [41].

Fig. 10 presents the flux trapping obtained on plain and perforated samples (36 mm in diameter and 15 mm in height) after conventional oxygenation at 450 °C for 150 hours. The samples (Fig. 4c) were previously magnetized at 1 T, 77 K, using an Oxford Inc. superconducting coil. The 3D representation of the magnetic flux shows the single dome in the both cases corresponding to the signature of a single-domain. The network of the holes has not affected the current loops at the large scale. This result was confirmed by the neutron diffraction measurements (D1B line at ILL, France) showing [52] only one single domain bulk orientation with mean c-axes parallel to the pellet axis. The trapped field value is higher in the perforated pellet (583 mT) than in the plain one (443 mT). This represents an increase of 32% for the drilled sample compared with the plain one, in agreement with our previous report [42]. This increasing of the trapped field value is probably due to: (i) better oxygenation and/or less cracks and porosities for the drilled pellet, as illustrated by Fig. 3b, (ii) strong pinning, because the hole could be favourable to the vortices' penetration, (iii) enhancement of the cooling, because the sample with holes offers a large and favourable surface exchange into the liquid nitrogen bath.

On the other hand, pulse magnetization was used on the drilled and plain pellets. Both samples (16 mm diameter samples, 8 mm thick) were tested with a series of pulse magnetization experiments. A Helmholtz coil was used to generate a homogeneous magnetic field. The maximum amplitude of the magnetic field is 1 T and the raising time of the pulse was 1 ms while the decay time was 10 ms. After the pulse, the trapped field was mapped with a hall sensor probe at 0.5 mm above the sample. The result shows that for the application of a 1 T pulse the trapped field increases by up to 60% for a drilled pellet [44] as compared with to the plain one. This is an interesting result for such a form of new

geometry, demonstrating the ability of the textured Y123 with multiple holes to trap a high field.
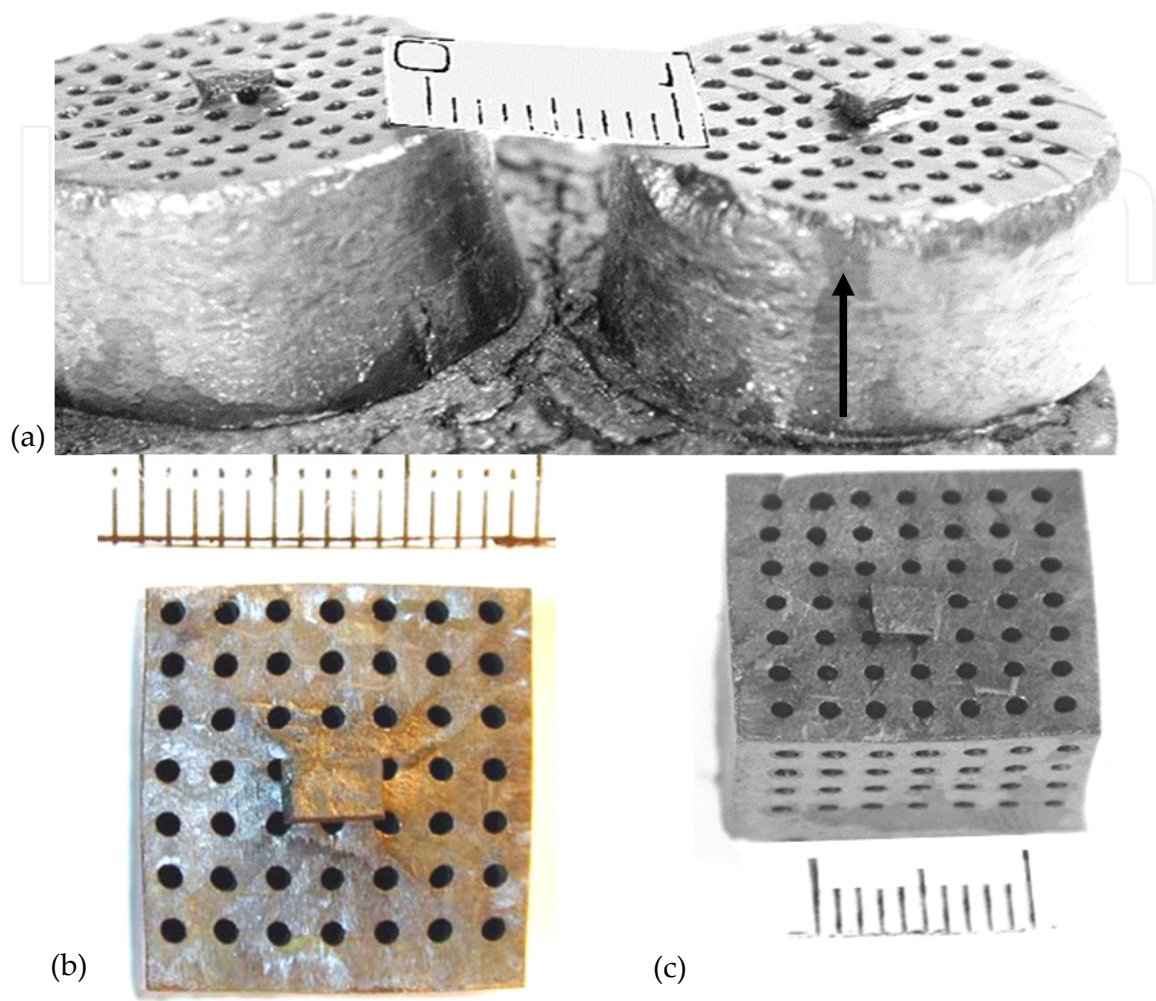

Figure 8. A batch of different as-grown drilled bulk samples (a) pellets, (b) square form and (c) interconnected samples.
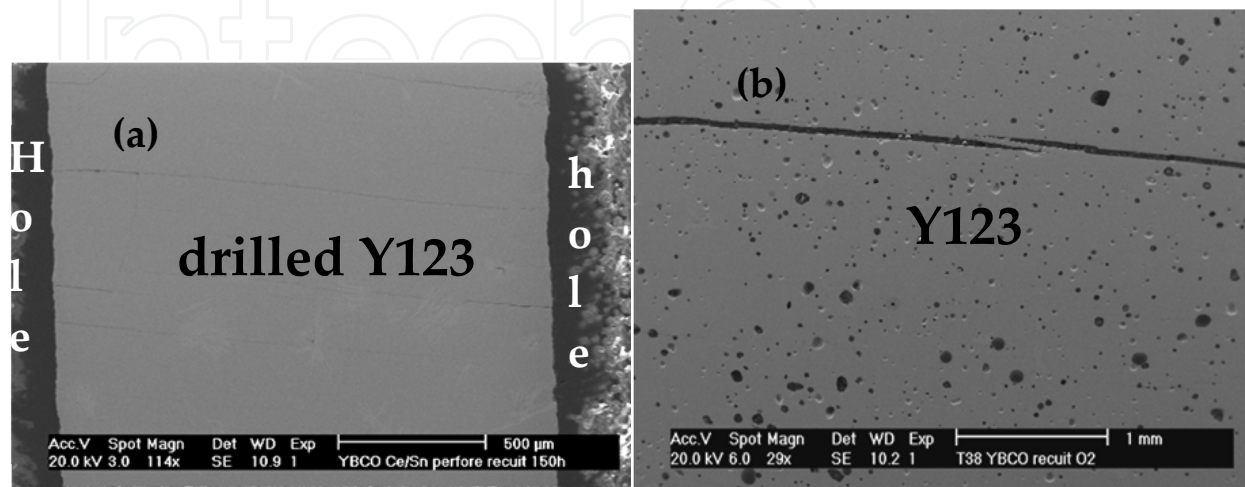

Figure 9. Microstructures of the (a) thin-wall and (b) plain samples, respectively.
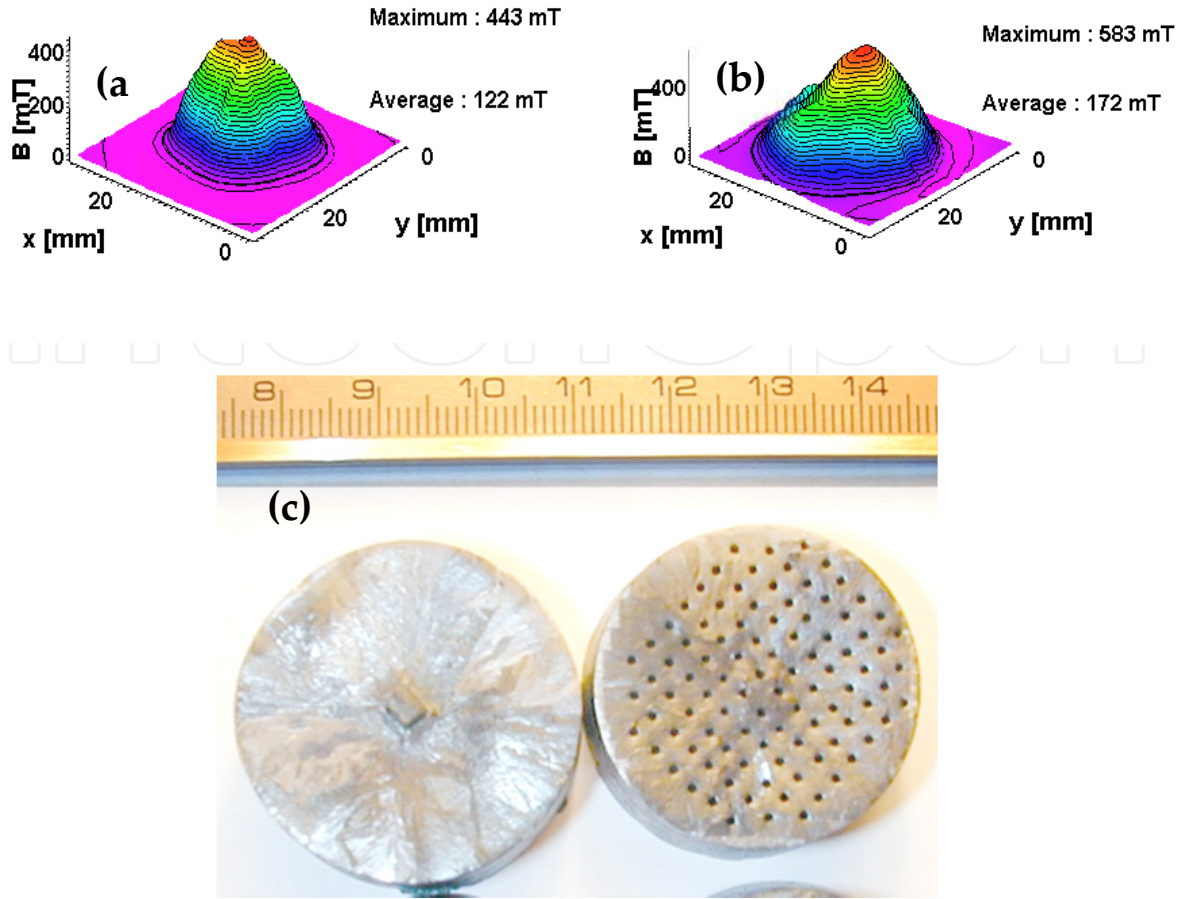
Figure 10. (a and b) Flux trapped measurements on (c) plain and multiple hole single domain pellets.

According to their thin wall geometry, the drilled bulk should be well oxygenated in comparison with the plain samples. The oxygen diffuses easily through the tube channels. The thermogravimetry technique was selected to compare the oxygenation quality of different pellets. The oxygen uptake was related to the increase of the sample weight. In this study, pellets of 16 and 24 mm diameter were used and a network of 30 holes was perforated. For each diameter, five drilled and five plain pellets were processed with the same heat treatment. All of the samples were weighted before and after the oxygenation, and the percentage of the weight gain was evaluated according to the following relation:

$$m \ (\%) = 100 \ (m_{final} - m_{initial})/m_{initial}$$

The measurements were realized twice to check reproducibility. For that, the samples after the first measurement were de-oxygenated at 900 °C, after half an hour, and followed by the quench step and then re-oxygenated. After the second measurement, the average values of the weight were estimated and plotted in Fig. 11. It was difficult to oxygenate the bulk sample with a big diameter and in this case the oxygen should diffuse into the core of the bulk. Generally, the big samples are annealed under oxygen at 400-450 °C between 150 to 600 hours [42, 46, 53, 54]. These annealing dwell times are so long in order to allow for oxygen diffusion until the core of the monolith bulk materials. The drilled samples seem to

offer an advantage (a saving of time) for annealing under oxygen of the superconductor bulk. This advantage is clearly shown in Fig. 11 where 25 hours is sufficient to obtain the full oxygenated sample; in the other word, maximum weight gain is quickly achieved. In addition, thin-wall geometry was introduced to reduce the diffusion paths and to enable a progressive oxygenation strategy [54]. As a consequence, cracks are drastically reduced. In addition, the use of a high oxygen pressure (16 MPa) further speeds up the process by displacing the oxygen–temperature equilibrium towards the higher temperature of the phase diagram. The advantage of thin-wall geometry is that such an annealing can be applied directly to a much larger sample during a shorter time (72 hrs compared with 150 hrs for the plain sample). Remarkable results have been obtained by the combination of thin walls and high oxygen pressure. Fig. 13 shows the 3D distribution of the trapped flux mapping measured at 77 K on the perforated thin wall pellet. The maximum trapped field value of 0.8 T is almost twice that obtained on the plain sample (0.33 T).
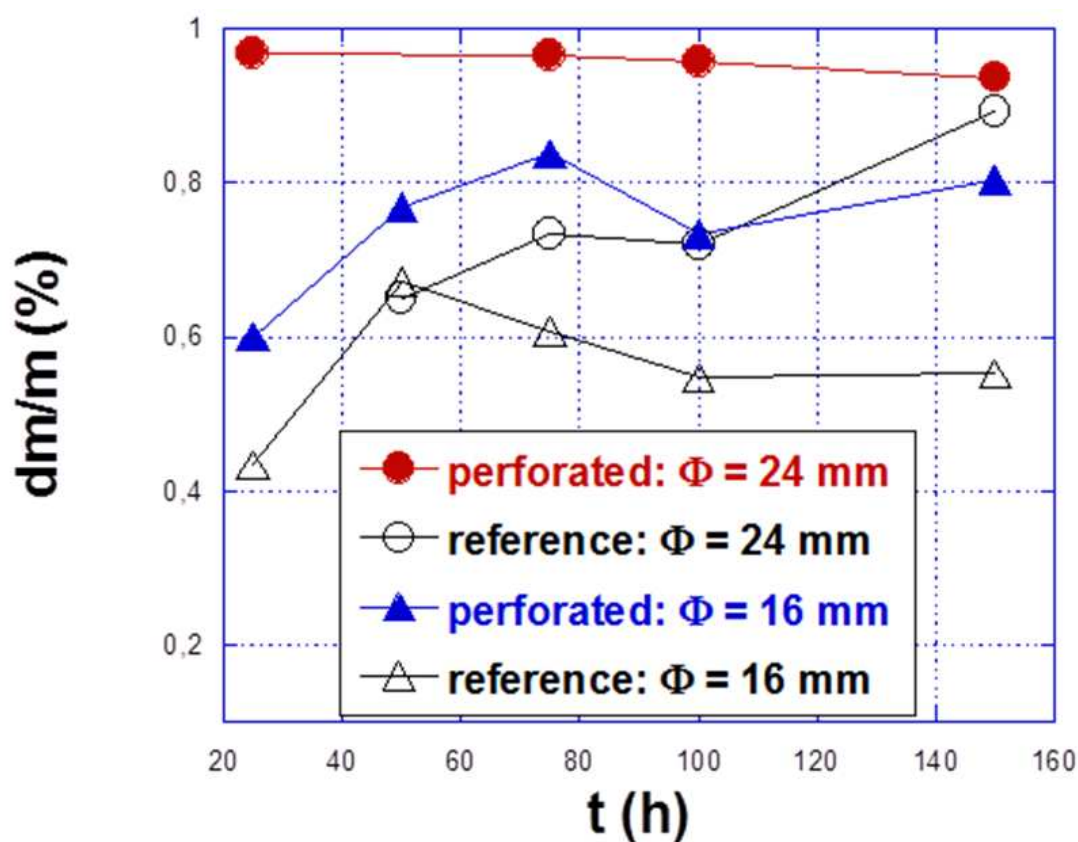

Figure 11. The influence of oxygen annealing on the oxygen uptake in the drilled and plain samples [44].

On the other hand, the effect of the number of the holes has been investigated and reported [56]. Table 1 summarizes the sample characteristics and the maximal trapped field values. We can clearly note that, for the samples having the same diameter and the same size of hole, the trapped field increases with the increase of the number of holes. An explanation could be that the better oxygenation is due to the large surface exchange with the density of the thin wall.

The Y123 domain with open holes could be reinforced, e.g. by infiltration with a low temperature melting alloy, so as to improve the mechanical properties that are useful for levitation applications or trapped field magnets. The perforated Y123 bulks with 1 or 2 mm diameter holes were dipped into the molten Sn/In alloy or an epoxy wax at 70 °C for 30 minutes in a vessel after evacuating it with a rotary pump and venting air to enable the molten alloy or liquid resin to fill up the holes. After cooling, the impregnated bulk materials were polished. Some samples were impregnated with a BiPbSnCd-alloy using the process described elsewhere [49]. Fig. 12 shows the top surface and the cross-sectional view of the impregnated Y123 bulk samples. We can see the dense and homogeneous infiltration of the wax epoxy and the Sn/In alloy. The magnetic flux mapping of the sample filled with a BiPbSnCd-alloy has been investigated. The same trapped field of 250 mT before and after impregnation has been measured. Presently, it is important to develop the specific shapes of bulk superconductors with mechanical reinforcement [52] for any practical application.
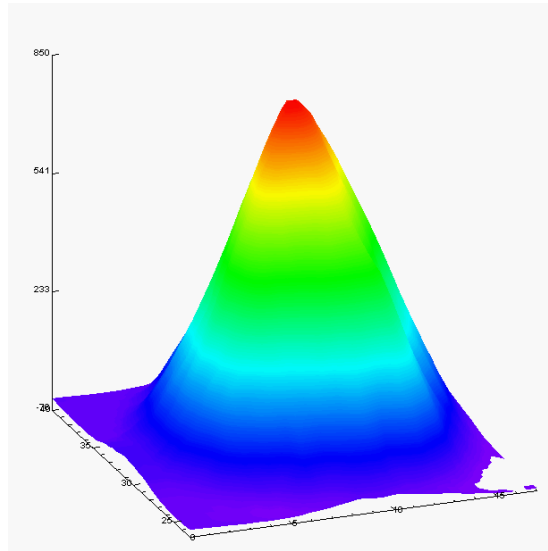

Figure 12. Flux-trapped measurements of the high pressure oxygenated thin wall sample.

sample ⌀ (mm)	20.8	20.7	20.7	20.6
sample thickness (mm)	7.6	7.6	7.8	7.5
number of holes	20	37	21	85
hole ⌀ (mm)	0.7	0.7	1.1	1.0
Bmax (T)	0.33	0.34	0.30	0.48

Table 1. Sample characteristics and maximal trapped field values in liquid nitrogen.

Multiple holes or porous ceramic materials, such as alumina and zirconia, are established components in a number of industrial applications such as inkjet printers, fuel injection systems, filters, structures for catalysts, elements for thermal insulation and flame barriers. The combination of a high specific surface with the ability to be reinforced in order to improve mechanical and thermal properties makes the perforated YBCO superconductors

interesting candidates both for a variety of novel applications and for fundamental studies. As an example, the artificial drilled Y123 in a desired structure [43, 57] is a good candidate for resistive elements in superconducting fault current limiters (FCL) [58, 59]. In this application, the thin wall between the holes allows more efficient heat transfer between a perforated superconductor and cryogenic coolant during an over-current fault compared with conventional bulk materials. The high surface area of the perforated materials, which may be adjusted by varying the hole diameter, makes them interesting candidates for studying fundamental aspects of flux pinning, since the extent of surface pinning, and hence J_c, are expected to differ significantly from bulk YBCO grains of a similar microstructure. This new structure has great potential for many applications with improved performance in place of Y123 hole-free bulks, since it should be easier to oxygenate and to maintain at liquid nitrogen temperature during application, avoiding the occurrence of hot spot. For meandering FCL elements, cutting is a crucial step as cracks appear during this stage. This can be solved by the *in situ* zigzag shape processing of holes, as we demonstrated the feasibility of elsewhere [43].
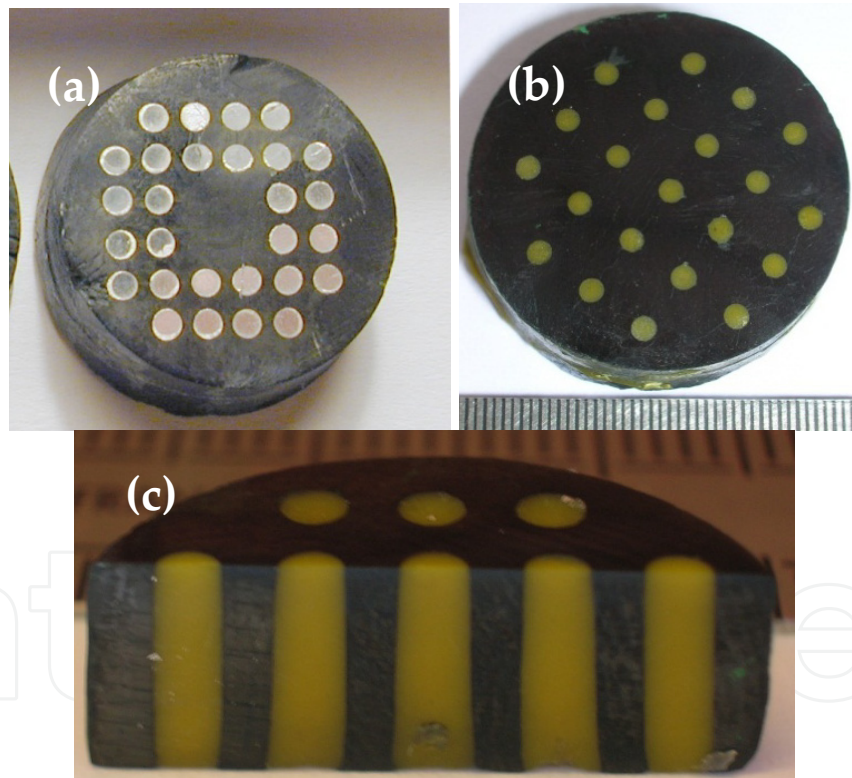

Figure 13. Reinforcement of the drilled samples. (a) The top view of the samples filled with a BiPbSnCd-alloy, (b) with wax resin and (c) a cross-section impregnated with wax resin.

Finally, we highlight the examples among recent progress of HTS bulk applications, flywheel, power devices as motors and generators, magnetic drug delivery systems and magnetic resonance devices as well.. As shown in Fig. 14, a variety of Gd123 bulks have been tested for the employment of field pole magnets as a way of intensifying flux trapping applications. The bulk magnets are cooled down to 30 K with step-by-step pulsed-field

magnetization using a homemade large dc current source. A large pulsed current is momentary applied to armature copper windings by which a pulsed magnetic field is formed and applied to the bulk field poles [60-63].

(a)   (b)

Figure 14. (a) A prototype bulk HTS motor designed for a specification of 30 kW 720 rpm and (b) a homemade pulsed-field magnetization system (TUMSAT-OLCR). This is an axial-type machine with a thermosyphon cooling system using Ne.

In summary, for the application of bulk HTS rotating machines, the enhancement of the trapped flux is a crucial task for achieving practical applications with high torque density. The increase of critical current density using artificial pinning centres marks an efficient technique for the enhancement of the properties of flux trapping. We attempted to enhance both the Jc and the trapped flux in bulk HTS with the addition of magnetic/ferromagnetic particles. An Fe-B-Si-Nb-Cr-Cu amorphous alloy was introduced into the Gd123 matrix. The melt growth of single-domain bulks with different magnetic particles was performed in air. The enhancement of the critical current density Jc at 77 K was derived in those bulks with the addition of Fe-B-Si-Nb-Cr-Cu, while the superconducting transition temperature of 93 K was not degraded significantly. The experiment of magnetic flux trapping was then conducted under static magnetic field magnetization with liquid nitrogen cooling. In the bulk with 0.4 mol% of Fe-B-Si-Nb-Cr-Cu, the integrated trapped flux exceeds over 35% compared with the one without the addition of magnetic particles. On the other hand, the addition of CoO particles resulted in a reduction of both Jc and trapped magnetic flux. The recent results indicate that the introduction of magnetic particles gives significant effect to the flux pinning's performance.

By inserting a buffer pellet with a higher T_p when compared with the matrix between the MgO seed and the bulk precursor, the lattice mismatch and low reactivity between the RE-Ba-Cu-O matrix and the MgO seed have been overcome. The undercooling and Gd211(Nd422) content for buffer pellet processing have systematically proven that the Gd-Ba-Cu-O and Nd-Ba-Cu-O bulks (16 mm in diameter) are successfully grown by this cold-seeding method. Cold-seeding melt-growth, not limited by the maximum temperature, is

realized by the present new method. It was demonstrated that the texture growth can be transferred from a high-T_P pellet to a low-T_P pellet, which may be promising for extending the growth window and processing large bulk superconductors.

The single domain of Y123 bulks with multiple holes has been processed and characterized. SEM investigations have shown that the holes' presence does not hinder the domain growth. The perforated samples exhibit a single domain character evidenced by a single dome trapped-field distribution and neutron diffraction studies. This new structure has great potential for many applications, with improved performances in place of Y123 hole free bulks, since it should be easier to maintain at liquid nitrogen temperature and/or to improve thermal conductivity during application, avoiding the appearance of hot spot. It is clear that the Y123 bulks with an artificial pattern of holes are useful for evacuating porosity from the bulk and assisting the uptake the oxygen. The ability of the Y123 material with multiple holes to trap a high field has been demonstrated. Using high pressure oxygenation, the trapped field increases up to 0.8 T at 77 K for the thin wall pellet, corresponding to 50% more than the bulk material without holes. Using pulse magnetization, the trapped fields increases by up to 60% for the drilled pellet with respect to the plain one. Superconducting bulks with an artificial array of holes can be filled with metal alloys or high strength resins to improve their thermal properties without any important decrease of the hardness [50], so as to overcome the built-in stresses in levitation and quasi-permanent magnet applications. The thin wall bulks superconducting on extruded shapes for portative permanent magnets are under development for the introduction at the large scale of this innovative approach of "material by design".

Author details

Mitsuru Izumi
TUMSAT-OLCR, Tokyo, Japan

Jacques Noudem
CRISMAT/LUSAC-UNICAEN, Caen, France

Acknowledgement

2. References

[1] Takizawa T and Murakami M Eds. (2005) Critical Current in Superconductors. Tokyo: Fuzambo International.

[2]   Matsushita T (2007) Flux Pinning in Superconductors. Berlin, Heidelberg New York: Springer.

[3]   Babu N H, Shi Y, Iida K and Cardwell D A (2005) *A practical route for the fabrication of large single-crystal (RE)–Ba–Cu–O superconductors*, Nat. Mater. 4: 476-480.

[4]   Cardwell D A, Shi Y, Babu N H, Pathak S K, Dennis A R and Iida K (2010) Top seeded melt growth of Gd–Ba–Cu–O single grain superconductors, Supercond. Sci. Technol. 23: 034008.

[5]   Cai C, Tachibana K and Fujimoto H (2000) Study on single-domain growth of Y$_{1.8}$Ba$_{2.4}$Cu$_{3.4}$O$_y$/Ag system by using Nd123/MgO thin film as seed, Supercond. Sci. Technol. 13: 698.

[6]   Oda M, Yao X, Yoshida Y and Ikuta H (2009) Melt-textured growth of (LRE)–Ba–Cu–O by a cold-seeding method using SmBa$_2$Cu$_3$O$_y$ thin film as a seed, Supercond. Sci. Technol. 22: 075012

[7]   Yao X, Nomura K, Nakamura Y, Izumi T and Shiohara Y (2002) Growth mechanism of high peritectic temperature Nd$_{1+x}$Ba$_{2-x}$Cu$_3$O$_{7-d}$ thick film on low peritectic temperature YBa$_2$Cu$_3$O$_{7-d}$ seed film by liquid phase epitax, J. Cryst. Growth 234: 611-615.

[8]   Li T, Cheng L, Yan S, Sun L, Yao X, Yoshida Y and Ikuta H (2010) Growth and superconductivity of REBCO bulk processed by a seed/buffer layer/precursor construction. Supercond, Sci. Technol. 23: 125002.

[9]   Muralidhar M, Tomita M, Suzuki K, Jirsa M, Fukumoto Y and Ishihara A (2010) A low-cost batch process for high-performance melt-textured GdBaCuO pellets, Supercond. Sci. Technol. 23: 045033.

[10]   Muralidhar M, Suzuki K, Ishihara A, Jirsa M, Fujumoto Y and Tomita M (2010) Novel seeds applicable for mass processing of LRE-123 single-grain bulks, Supercond. Sci. Technol. 23: 124003.

[11]   Kim C, Lee J, Park S, Jun B, Han S and Han Y (2011) Y$_2$BaCuO$_5$ buffer block as a diffusion barrier for samarium in top seeded melt growth processed YBa$_2$Cu$_3$O$_{7-y}$ superconductors using a SmBa$_2$Cu$_3$O$_{7-d}$ seed, Supercond. Sci. Technol. 24: 015008.

[12]   Zhou D, Xu K, Hara S, Li B, Deng Z, Tsuzuki K and Izumi M (2012) MgO buffer-layer-induced texture growth of RE–Ba–Cu–O bulk, Supercond. Sci. Technol. 25: 025002.

[13]   Xu Y, Izumi M, Tsuzuki K, Zhang Y, Xu C, Murakami M, Sakai N and Hirabayashi I (2009) Flux pinning properties in a GdBa$_2$Cu$_3$O$_{7-\delta}$ bulk superconductor with the addition of magnetic alloy particles, Supercond. Sci. Technol. 22: 095009.

[14]   Xu C, Hu A, Sakai N, Izumi M and Hirabayashi I (2005) Effect of BaO$_2$ and fine Gd$_2$BaCuO$_{7-\delta}$ addition on the superconducting properties of air-processed GdBa$_2$Cu$_3$O$_{7-\delta}$, Supercond. Sci. Technol. 18: 229-233.

[15]   Cardwell D A, Babu N H, Lo W and Campbell A M (2000) Processing, microstructure and irreversibility of large-grain Nd-Ba-Cu-O, Supercond. Sci. Technol. 13: 646-651.

[16]   Babu, N H and Lo, W and Cardwell, D A and Shi, Y H (2000) *Fabrication and microstructure of large grain Nd-Ba-Cu-O.* Superconductor, Science and Technology, 13: 468-472.

[17]   Cima M, Flemings M, Figueredo A, Nakade M, Ishii H, Brody H and Haggerty J (1992) Semisolid solidification of high temperature superconducting oxides, J. Appl. Phys. 72: 179-191.

[18]   Ishii Y, Shimoyama J, Tazaki Y, Nakashima T, Horii S and Kishio K (2006) Enhanced flux pinning properties of YBa$_2$Cu$_3$O$_y$ by dilute impurity doping for CuO chain, Appl. Phys. Lett. 89: 202514-202517.

[19] Hari Babu N, Shi Y, Pathak S K, Dennis A R and Cardwell D A (2011) Developments in the processing of bulk (RE)BCO superconductors, Physica C 471: 169-178.

[20] Hari Babu N, Reddy E S, Cardwell D A, Campbell A M, Tarrant C D and Schneider K R (2003) Artificial flux pinning centers in large, single-grain (RE)-Ba-Cu-O superconductors, Appl. Phys. Lett. 83: 4806-4809.

[21] Muralidhar M, Sakai N, Jirsa M, Murakami M and Hirabayashi I (2008) Record flux pinning in melt-textured NEG-123 doped by Mo and Nb nanoparticles, Appl. Phys. Lett. 92: 162512-162515.

[22] Hu A, Xu C, Izumi M, Hirabayashi I and Ichihara M (2006) Enhanced flux pinning of air-processed $GdBa_2Cu_3O_{7-\delta}$ superconductors with addition of ZrO_2 nanoparticles, Appl. Phys. Lett. 89: 192508-192511.

[23] Xu C, Hu A, Ichihara M, Izumi M, Xu Y, Sakai N and Hirabayashi I (2009) Transition electron microscopy and atomic force microscopy observation of Air-Processed $GdBa_2Cu_3O_{7-\delta}$ superconductors doped with metal oxide nanoparticles (Metal = Zr, Zn, and Sn) , Jpn. J. Appl. Phys. 48: 023002.

[24] Muralidhar M, Sakai N, Jirsa M, Koshizuka N, Murakami M, (2004) Direct observation and analysis of nanoscale precipitates in $(Sm,Eu,Gd)Ba_2Cu_3O_y$, Appl. Phys. Lett. 85: 3504-3507.

[25] Xu Y, Izumi M, Tsuzuki K, Zhang Y, Xu C, Murakami M, Sakai N, Hirabayashi I (2009) Flux pinning properties in a $GdBa_2Cu_3O_{7-\delta}$ bulk superconductor with the addition of magnetic alloy particles, Supercond. Sci. Tech. 22: 095009.

[26] Xu K, Tsuzuki K, Hara S, Zhou D, Zhang Y, Murakami M, Nishio-Hamane D, Izumi M, (2011) Microstructural and superconducting properties in single-domain Gd–Ba–Cu–O bulk superconductors with in situ formed Fe_3O_4 ferrimagnetic particles, Supercond. Sci. Tech. 24: 085001.

[27] Xu C, Hu A, Sakai N, Izumi M and Hirabayashi I, (2006) Flux pinning properties and superconductivity of Gd-123 superconductor with addition of nanosized SnO_2/ZrO_2 particles, Physica C 445: 357-360.

[28] Yamazaki Y, Akasaka T, Ogino H, Horii S, Shimoyama J and Kishio K (2009) Excellent Critical Current Properties of Dilute Sr-Doped Dy123 Melt-Solidified Bulks at Low Temperatures, IEEE Trans. Appl. Supercond. 19: 3487-3490.

[29] Xu C, Hu A, Ichihara M, Sakai N, Hirabayashi I and Izumi M, (2007) Role of ZrO_2/SnO_2 Nano-Particles on Superconducting Properties and Microstructure of Melt-Processed Gd123 Superconductors, IEEE Trans. Appl. Supercond. 17: 2980-2983.

[30] Muralidhar M, Jirsa M and Tomita M, (2010) Flux pinning and superconducting properties of melt-textured NEG-123 superconductor with TiO_2 addition, Physica C 470: 592-597.

[31] Hari Babu N, Iida K and Cardwell D A (2007) Flux pinning in melt-processed nanocomposite single-grain superconductors, Supercond. Sci. Technol. 20: S141.

[32] Nariki S, Sakai N and Murakami M (2002) Development of Gd–Ba–Cu–O bulk magnets with very high trapped magnetic field, Physica C 378-381: 631-635.

[33] Nariki S, Sakai N, Murakami M and Hirabayashi I (2004) High critical current density in RE–Ba–Cu–O bulk superconductors with very fine RE_2BaCuO_5 particles, Physica C 412-414: 557-565.

[34] Gilligns W, Sihanek A V and Moshchalkov V V (2007) Superconducting microrings as magnetic pinning centers, Appl. Phys. Lett. 91: 202510-202513.

[35] Blamire M G, Dinner R B, Wimbush S C and MacManus-Driscoll J L (2009) Critical current enhancement by Lorentz force reduction in superconductor–ferromagnet nanocomposites, Supercond. Sci. Technol. 22: 025017.

[36] Wimbush S C, Durrell J H, Bali R, Yu R, Wang H Y, Harrington S A and MacManus-Driscoll J L (2009) Practical Magnetic Pinning in YBCO, IEEE Transactions on Appl. Supercond. 19: 3148.

[37] Wimbush S C, Durrell J H, Tsai C F, Wang H, Jia Q X, Blamire M G and MacManus-Driscoll J L (2010) Enhanced critical current in YBa$_2$Cu$_3$O$_{7-\delta}$ thin films through pinning by ferromagnetic YFeO$_3$ nanoparticles, Supercond. Sci. Technol. 23: 045019.

[38] Xu K, Tsuzuki K, Hara S, Zhou D, Xu Y, Nishio-Hamane D and Izumi M, (2011) Enhanced Flux Pinning and Microstructural Study of Single-Domain Gd-Ba-Cu-O Bulk Superconductors With the Addition of Fe-Containing Alloy Particles, IEEE Trans Magnetics. 47: 4139-4142.

[39] Tsuzuki K, Hara S, Xu Y, Morita M, Teshima H, Yanagisawa O, Noudem J, Harnois C and Izumi M, (2010) Enhancement of the Critical Current Densities and Trapped Flux of Gd-Ba-Cu-O Bulk HTS Doped With Magnetic Particles, IEEE Trans. Appl. Supercond. 21: 2714-2717.

[40] Xu Y, Tsuzuki K, Hara S, Zhang Y, Kimura Y and Izumi M, (2010) Spatial variation of superconducting properties of Gd123 bulk superconductors with magnetic particles addition, Physica C 470: 1219-1223.

[41] Meslin S, Harnois C, Chateigner D, Ouladdiaf B, Chaud X, Noudem J G (2005) Perforated monodomain YBa$_2$Cu$_3$O$_{7-x}$ bulk superconductors prepared by infiltration-growth process. Journal of the European Ceramic Society 25: 2943-2946.

[42] Chaud X, Meslin S, Noudem J, Harnois C, Porcar L, Chateigner D, Tournier R (2005) Isothermal growth of large YBaCuO single domains through an artificial array of holes, J. of Crystal Growth 275: e855-e860.

[43] Noudem J, Meslin S, Harnois C, Chateigner D and Chaud X (2004) Melt textured YBa$_2$Cu$_3$O$_y$ bulks with artificially patterned holes: a new way of processing c-axis fault current limiter meanders, Supercond. Sci. Technol. 17: 931.

[44] Noudem J, Meslin S, Horvath D, Harnois C, Chateigner D, Eve S, Gomina M, Chaud X and Murakami M (2007) Fabrication of textured YBCO bulks with artificial holes, Physica C 463–465: 301–307.

[45] Chaud X, Noudem J, Prikhna T, Savchuk Y, Haanappel E, Diko P and Zhang C (2009) Flux mapping at 77 K and local measurement at lower temperature of thin-wall YBaCuO single-domain samples oxygenated under high pressure, Physica C 469: 1200–1206.

[46] Isfort D, Chaud X, Tournier R and Kapelski G (2003) Cracking and oxygenation of YBaCuO bulk superconductors: application to c-axis elements for current limitation, Physica C 390: 341.

[47] Diko P, Fuchs G and Krabbes G (2001) Influence of silver addition on cracking in melt-grown YBCO, Physica C 363: 60.

[48] Noudem J, Tarka M and Schmitz G (1999) Preparation and characterization of electrical contacts to bulk high-temperature superconductors, Inst. Phys. Conf. Ser. No 167, EUCAS, Spain, 14-17 September: 183.

[49] Tomita M and Murakami M (2003) High-temperature superconductor bulk magnets that can trap magnetic fields of over 17 tesla at 29 K, Nature 421: 517.

[50] Fuchs G, Gruss S, Verges P, Krabbes G, Muller K, Fink J and Schultz L (2002) High trapped fields in bulk YBCO encapsulated in steel tubes, Physica C 372-376: 1131.

[51] Krabbes G, Fuchs G, Schatzle P, Gruss S, Park J, Hardinghaus F, Hayn R and Drechsler S-L (2000) YBCO - monoliths with trapped fields more than 14 T and peak effect, Physica C 341-348: 2289-2292.

[52] Noudem J, Meslin S, Horvath D, Harnois C, Chateigner D, Ouladdiaf B, Eve S, Gomina M, Chaud X and Murakami M (2007) Infiltration and Top Seed Growth-Textured YBCO Bulks With Multiple Holes, J. Am. Ceram. Soc. 90: 2784-2790.

[53] Diko P, Kracunovska S, Ceniga L, Bierlich J, Zeiberger M and Gawalek W (2005) Microstructure of top seeded melt-grown YBCO bulks with holes, Supercond. Sci. Technol. 18: 1400.

[54] Nariki S, Sakai N, Murakami M (2005) Melt-processed Gd-Ba-Cu-O superconductor with trapped field of 3 T at 77 K, Supercond. Sci. Technol. 18: S126.

[55] Chaud X, Noudem J, Prikhna T, Savchuk Y, Haanappel E, Diko P and Zhang C (2009) Flux mapping at 77 K and local measurement at lower temperature of thin-wall YBaCuO single-domain samples oxygenated under high pressure, Physica C 469: 1200-1206.

[56] Haindl S, Hengstberger F, Weber H, Meslin S, Noudem J and Chaud X (2006) Hall probe mapping of melt processed superconductors with artificial holes, Supercond. Sci. Technol. 19: 108-115.

[57] Harnois C, Meslin S, Noudem J, Chateigner D, Ouladdiaf B and Chaud X (2005) Shaping of melt textured samples for fault current limiters, IEEE Trans. Appl. Supercond. 15: 3094.

[58] Tournier R, Beaugnon E, Belmont O, Chaud X, Bourgault D, Isfort D, Porcar L and Tixador P (2000) Processing of large $Y_1Ba_2Cu_3O_{7-x}$ single domains for current-limiting applications, Supercond. Sci. Technol. 13: 886.

[59] Tixador P, Obradors X, Tournier R, Puig T, Bourgault D, Granados X, Duval J, Mendoza E, Chaud X, Varesi E, Beaugnon E and Isfort D (2000) Quench in bulk HTS materials - application to the fault current limiter, Supercond. Sci. Technol. 13: 493.

[60] Tsuzuki K, Hara S, Xu Y, Morita M, Teshima H, Yanagisawa O, Noudem J, Harnois Ch. Izumi M (2011) Enhancement of the Critical Current Densities and Trapped Flux of Gd-Ba-Cu-O Bulk HTS Doped With Magnetic Particles, IEEE Trans. Appl. Supercond. 21: 2714-2717.

[61] Miki M, Felder B, Tsuzuki K, Deng Z, Shinohara N, Izumi M, Ida T and Hayakawa H (2011) Influence of AC Magnetic Field on a Rotating Machine With Gd-Bulk HTS Field-Pole Magnets, IEEE Trans. Appl, Supercond. 21: 1185-1189.

[62] Morita E, Matsuzaki H, Kimura Y, Ogata H, Izumi M, Ida T, Murakami M, Sugimoto H and Miki M (2006) Study of a new split-type magnetizing coil and pulsed field magnetization of Gd–Ba–Cu–O high-temperature superconducting bulk for rotating machinery application, *Supercond. Sci. Technol.* 19: 1259.

[63] Miki M, Felder B, Tsuzuki K, Xu Y, Deng Z, Izumi M, Hayakawa H, Morita M and Teshima H, (2010) Materials processing and machine applications of bulk HTS, Supercond. Sci. Technol. 23:124001.